CFD Study of the Normal Force Exerted on a Sphere Moving Close to a Surface

Asem AL Jarrah
Natural Resources and Chemical Engineering Department, Tafila Technical University, Tafila, Jordan.

Abstract-

The normal force exerted on a sphere moving close to a surface, or what so called the wall-force, is an important force in modeling multiphase flow as well as in understanding the hydrodynamic behavior of moving an object close to a surface. The current widely spread models for thewall-force are based on derivations that relayon the potential flow theory, which ignore the effect of viscosity. Moreover, these current models always represent the wall face as a repulsive force, which is not the case as this study shows. In this study the wall-force was studiedusing Fluent Software Package and a relatively simple CFD-based correlation for the wall force was developed. The study shows that the wall force decrease rapidly as the distance of the sphere from the surface increases reaching zero at a distance of about half the diameter of the sphere then this force becomes weekly negative, attractive rather than repulsive, as the distance increases further. The wall force remains attractive untilapproximately the distance reachesfourtimes the diameter of the sphere and then becomes and remainszero as the distance increase further.

Keywords*:Wall Force, Normal Force, Sphere, Fluent Software Package, CFD.*

I. INTRODUCTION

When a sphere moves in close proximity to a surface, the normally uniform flow of the liquid around the sphere changes dramatically. The no-slip condition at the wall slows the liquid velocity between the sphere and the wall which in turn, relatively, increases the liquid velocity of the opposite side. The net effect of this asymmetry is a force which acts to drive the sphere away from the wall. This force, which is usually called the wall force, is important in many applications,especially in multiphase flow such as gas-liquid bubbly flowor solid-liquid flow. Understanding this force is essential to explain the behavior of the bubbles near the wall. The wall force, which is normal to the surface,wasmodeled based on the potential flow theory by a widely spread model developed byAntal [1, 1991]:

$$F_w = \frac{\pi}{6}\rho d^2 v^2 \left[-0.208 + 0.147\left(\frac{d}{y}\right)\right] \quad (1)$$

This model was widely accepted and used in the literaturefor the wall force, De Bertodano et. al. [2, 1994], Troshko and Hassan [3, 2001], and Tomiyamaa, et. al. [4,2002]. Later this model for the wall force was modifiedbyLucasa et. al. [5, 2007]and Rzehak et. al. [6, 2012] as

$$F_w = \begin{cases} \frac{\pi}{6}\rho d^2 v^2 \left[-0.208 + 0.147\left(\frac{d}{y}\right)\right] & for\ \frac{208}{147} \geq \frac{d}{y} \\ 0 & for\ \frac{208}{147} < \frac{d}{y} \end{cases} \quad (2)$$

The modification in equation 2 was justified to the reason that when the sphere moves far from the wall, the wall force cannot be negative as equation 1 predicts, and therefore, should be zero. This justification has no theoretical basis. The objective of this research is to clear out the argument about this point, explain the possibility of negative wall force,derive a CDF-based correlationmodel for the wall forcethat account for the effect of viscosity (i.e., the solution of the Nervier-Stocks equation rather than the potential flow solution), compare magnitudes of wall force to drag force, and validate the model via published experimental data.

II. RESULTS AND DISCUSSION

A. *Modeling the Wall Force*

Fluent version 6.3 software package was used to study the wall force. Laminar flow was assumed in this studyand water at 25 ^{o}C and 1 atm was used as the working fluid. The wall force was studied versus the dimensionless ratio y/d, the distance to diameter ratio. Gambit version 2.4.6 software package was used for the meshing.Triangular elements with a size function near the wall and around the sphere were used in the meshing in orderto capture the details of the boundary layers. Figure 1 shows the type of meshing used for the cases of y/d=0 and y/d=1.

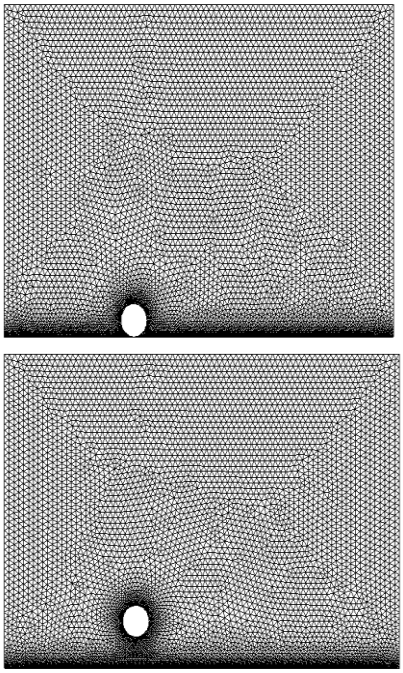

Figure 1: The Type of meshing used in this Study for the Cases of y/d=0 and y/d=1.

Table 1 shows the obtained results for the simulation. The pressure force, the viscous force, and the total force with their coefficientswere computed at various values of y/d at constant Reynolds number.

y/d	Press. Force (N)	Vis. Force (N)	Total Force (N)	Press. Coeff.	Vis. Coeff.	Total Coeff.
0.0	113.9	0.292	114.2	186.0	0.478	186.5
0.1	39.15	0.221	39.37	63.92	0.360	64.28
0.4	1.134	0.057	1.191	1.851	0.093	1.944
0.7	-6.350	0.050	-6.300	-10.38	0.082	-10.29
1.0	-6.048	0.048	-6.000	-9.874	0.079	-9.796
1.2	-5.335	0.335	-5.000	-8.710	0.548	-8.163
1.5	-4.020	0.020	-4.000	-6.563	0.033	-6.530
2.0	-3.238	0.034	-3.204	-5.286	0.056	-5.231
3.0	-2.045	0.045	-2.001	-3.339	0.074	-3.265
4.0	0.000	0.000	0.000	0.000	0.000	0.000

Table 1: Wall Normal Forces Versus the Dimensionless Quantity y/d.

Figure 2 shows some velocity contours for this study. In order to compare magnitude of forces, the drag force coefficient of the sphere was also computed and compared with the wall force as shown in Figure 3.Moreover, Figure 3 shows the force coefficient for the drag force and for the wall force plotted versus y/d. It can be seen that the drag force is approximately constant while the wall force is relatively high in the region very close to the wall. The wall force decreases rapidly to zeroas

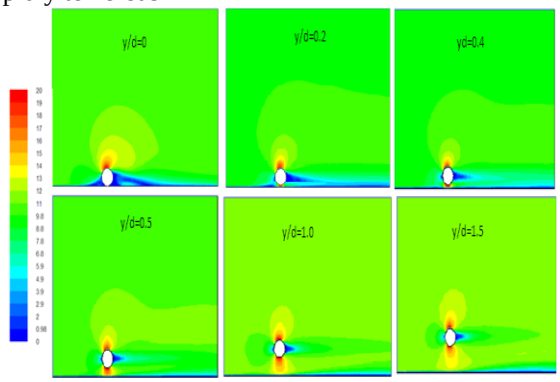

Figure 2: Velocity Contours for selected y/d (The colormap is in m/s).

the distance increase, then becomes negative as the distance increase further, and then returns back to zero as the sphere distance from the surface becomes large.

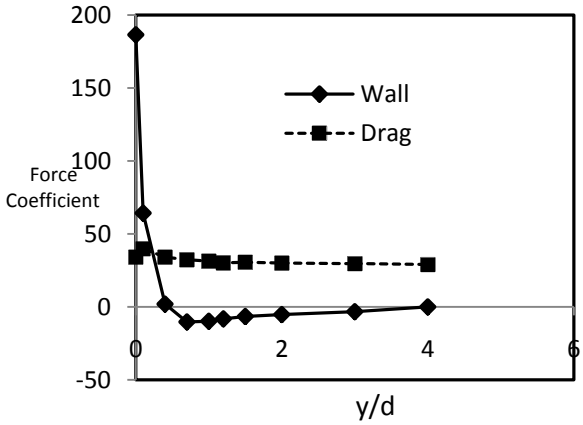

Figure 3: Wall Force Coefficient and Drag Force Coefficient Versus y/d.

The wall force coefficient versus y/d (data of Table 1) was correlated by the following correlation:

$$\frac{Wall\ Force}{A\left(\frac{1}{2}\rho v^2\right)} = \begin{cases} -402.9\frac{y}{d} + 151.4 & \text{for } 0 \le \frac{y}{d} < 0.4 \\ 70.667\frac{y}{d} - 118.5\frac{y}{d} + 38.037 & \text{for } 0.4 \le \frac{y}{d} \le 1 \\ 2.9632\frac{y}{d} - 11.77 & \text{for } 1 \le \frac{y}{d} < 4 \\ 0 & \text{for } 4 \le \frac{y}{d} \end{cases} \quad (3)$$

B. Model Validation

The model derived for the wall was validated against published data by H. Monji, B. Oesterle, P. Boulet, G. Matsui [7]. The Lagrangian-Eulerian approach was used to model the flow as follows [8]:

Particles continuity:

$$\frac{\partial}{\partial t}(\rho_p \alpha_p) + \nabla.(\rho_p \alpha_p \vec{v}) = 0 \quad (4)$$

Particles momentum:

$$\rho_p V_p \frac{D\vec{v}}{Dt} = \rho_p V_p \vec{g} + V_p \overrightarrow{\Delta P} + \overrightarrow{F_D} + \overrightarrow{F_l} + \overrightarrow{F_w} + \overrightarrow{F_{td}} \quad (5)$$

Liquid continuity:

$$\frac{\partial}{\partial t}(\rho_l \alpha_l) + \nabla.(\rho_l \alpha_l \vec{u}) = 0 \quad (6)$$

Liquid momentum:

$$\frac{\partial(\alpha_p \rho_p \vec{v} + \alpha_l \rho_l \vec{u})}{\partial t} = -\nabla.(\alpha_p \rho_p \vec{v}\vec{v} + \alpha_l \rho_l \vec{u}\vec{u}) - \nabla(\alpha_l \bar{\bar{\tau}}) - \nabla P + (\alpha_p \rho_p + \alpha_l \rho_l)\vec{g} \quad (7)$$

The influence of the liquid phase turbulence on the particle motion is simulated by means of the well-known eddy-particle interaction model [9] through generating liquid velocity fluctuations, according to the local turbulent intensity, which are kept constant during the duration of interaction between the discrete particle and the corresponding fluid particle. Collisions between particles and between a particle and the pipe wall was also considered. Such collisions are treated according to Tsuji *et al*. [10] by means of momentum conservation. The parameters needed for collision processing are the coefficient of restitution and the coefficients of static and kinetic friction. The time step for particle trajectory calculation is chosen as 1/10 of the average time interval between two particle-particle collisions. The liquid turbulence was predicted using *k*-ε model [11,12]. Fluent 6.3 software package was used to solve the model and the user defined function was used to define the forces.

The pressure drop of the published data at the test section was measured for each particle size with changing the total flow rate Qt and particle weight concentration Cw. In order to compare the pressure loss among the results under different conditions, a ratio of the additional pressure loss by particles to the pressure loss of the single-phase flow, R, was introduced as:

$$R = \frac{\left(\frac{dP}{dZ}_{two\ -phase}\right) - \left(\frac{dP}{dZ}_{single\ -Phase}\right)}{\left(\frac{dP}{dZ}_{single\ -phase}\right)} \quad (8)$$

Where $\left(\frac{dP}{dZ}_{single\ -Phase}\right)$ and $\left(\frac{dP}{dZ}_{two\ -phase}\right)$ are the pressure losses of a water single-phase flow and a two-phase flow having the same total flow rate, respectively.Figures 4-6 show the ratio of the additional pressure loss, R, for the particle concentration. The numerical result agrees well with the experimental data.Figure 4 shows the case of the particle size D = 0.5 mm. The experimental results shows that the ratio of the additional pressure loss was positive for all cases and increased with the particle concentration Cw and deceased with the flow rate Qt. Figure 5 shows the case of D=1mm. The results show the ratio of the additional pressure loss decreased with the flow rate Qt, as well as the case of D=0.5mm. The ratio of the additional pressure loss, however, was negative under the conditions of Qt=15, 20 L/min and small particle concentration. The negative ratio of additional pressure loss suggests that the pressure loss of two-phase flow is smaller than that of the water single phase flow, that is, pressure drop reduction phenomena in the two-phase flow.

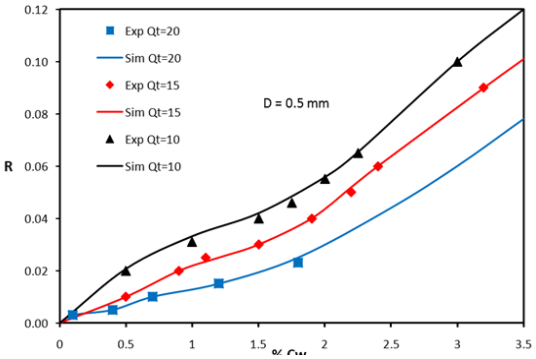

Figure 4: Comparison Between the Experimental Values and the Calculated Values of the Additional Pressure Loss Ratio vs, Particles Weight Concentration for D = 0.5 mm.

The ratio of the additional pressure loss increased with the particle concentration and changed to positive. In the case of Qt=20 L/min, the negative minimum value of R was smaller and the transition concentration from the negative to the positive was larger comparing with those in the case of Qt=15 L/min.

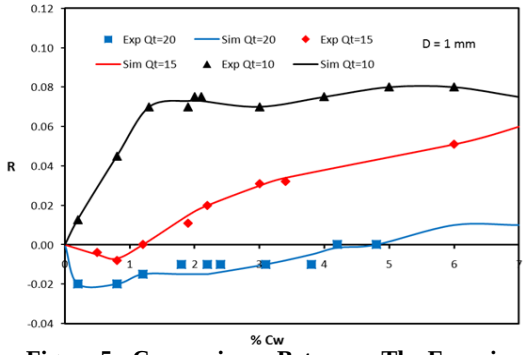

Figure 5: Comparison Between The Experimental Values and the Calculated Values of the Additional Pressure Loss Ratio Vs, Particles Weight Concentration For D = 1 Mm.

Figure 6 shows the case of D=1.5 mm, the ratio of the additional pressure loss take a negative values in all its range for case of Qt= 20 L/min. In general, based on the results shown in Fig. 3, the ratio of the additional pressure loss take negative values under the conditions of D=1 and 1.5 mm, high velocity and low concentration.

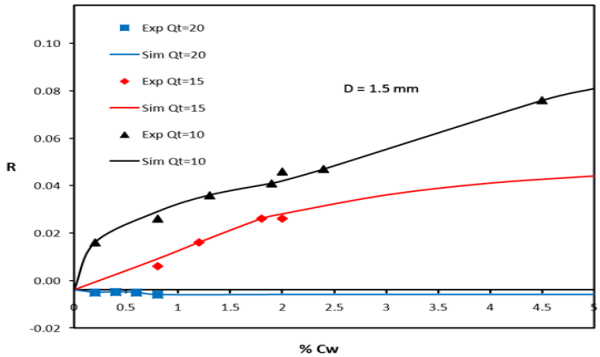

Figure 6: Comparison Between the Experimental Values and the Calculated Values of the Additional Pressure Loss Ratio vs. Particles Weight Concentration for D = 1.5 mm.

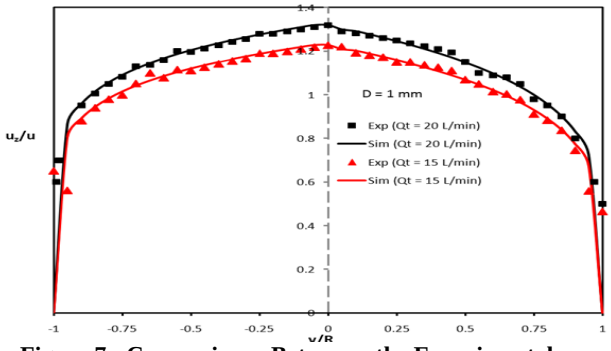

Figure 7: Comparison Between the Experimental Values and the Calculated Values of the Velocity Profile Along the Pipe Diameter for D =1 Mm.

Figures 7-9 show the z-direction velocity distribution on the y-axis, that is, the radial distribution of the main flow velocity along the gravitational direction. The flow velocity u_z and y-position are normalized by the average velocity u on the cross section and the pipe radius R, respectively. The flows were very dilute. The weight concentration of the flow was 0.48 wt% for the particle size D= 0.5 mm, 0.12 wt% for the particle size D= 1.0 mm and 1.1 wt% for the particle size D= 1.5 mm.

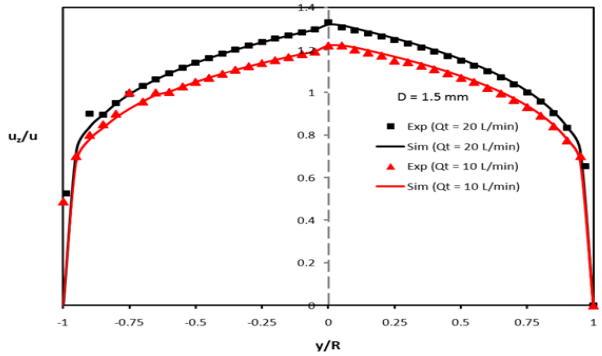

Figure 8: Comparison Between the Experimental Values and the Calculated Values of the Velocity Profile Along the Pipe Diameter for D =1.5 Mm.

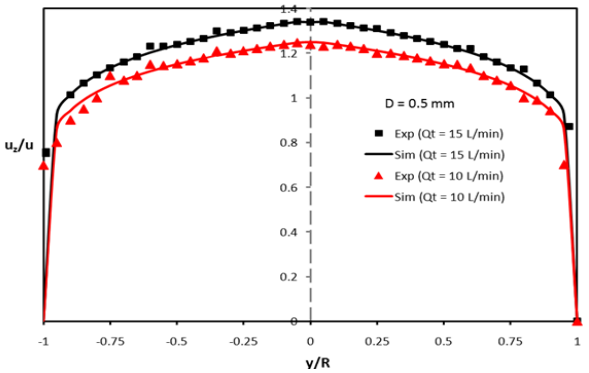

Figure 9: Comparison Between the Experimental Values and the Calculated Values Of The Velocity Profile Along the Pipe Diameter for D = 0.5 Mm.

Figure 7 shows the velocity profiles for the low flow rate Qt=10 L/min. The velocity profiles of the two-phase flow were not symmetrical to the pipe axis. In the lower part of the pipe, the water velocity increases while it decreases in the upper part. The velocity near the upper wall was also slightly high for the particle of D= 0.5 mm comparing with the case of the particle of D= 1.0 mm. The difference of the velocity distribution is caused by the distribution of the particle concentration.

Considering the wall shear stress caused by the velocity gradient, the wall shear stress by the two-phase flow is higher in the lower part and lower in the upper

part of the pipe comparing with the water single phase flow. The total pressure loss depends on the integration of the wall shear stress. In the small particle case, the velocity gradient near the upper wall was large and the shear stress was also high. Therefore, the pressure loss was larger than that of the water single phase flow. For the cases of D = 1 mm and 1.5 mm, the shear stress at the upper wall decreases and totally the pressure loss decreases. The flow was three-dimensional and the velocity profile and the shear stress should be discussed on the three-dimensional distribution.

III. CONCLUSIONS

In this work the normal force exerted by a surface on a sphere moving close to the surface was studied. The results show that the wall force is comparable to the drag force on the sphere. In the very close to the wall region, the wall force is several times larger than the drag force. As the distance from the wall increase, the wall force decreases while the drag force remains approximately constant at constant Reynolds number. Moreover,the study shows thata negative force on the sphere (i.e., attractive force rather than a repulsive force) is possible, but very small.The results also show that, the wall force decrease rapidly as the sphere distance from the wall increase reaching zero at a distance of about half the diameter of the sphere then this force becomesnegative until the distance becomes about four times the diameter of the spherethen this force return back to zero. The negative force (the attraction of the sphere to the wall) in the range of $0.5 \leq y/d \leq 4$ isdue to the increase in the velocity of the fluid between the sphere and the surface (as seen clearly in Figure 2). This velocity increase is dueto the boundary layers on the surface of the wall and on the surface of the sphere, the boundary layers slows the fluid velocity on the surface of the sphere and wall, which in turn increase the velocity in the region between the surface and sphere to maintain continuity. This increase in velocity causes the pressure between the sphere and the wall to be larger than the pressure above the sphere. This pressure difference is the cause of the negative force (the attractive force). However, this attractive force as it seen in Figure 3 is very small and safely can be ignored.

Nomenclature

A Sphere Projection Area [m^2]
v Velocity [m/s]
y Sphere Distance from the Wall
d Sphere Diameter[m]
F_wWall Force
$C_d$drag coefficient [-]
D average diameter of particles [m]
g acceleration of gravity [m/s^2]
R ratio of additional pressure drop to single-phase pressure drop [-]
z coordinate along pipe axis [m]
y distance from the center of the pipe [m]
v, particle velocity [m/s]
u, liquid velocity [m/s]
Vp volume of a particle [m^3]
P pressure [Pa]
z coordinate along pipe axis [m]
F force [N]
Re Reynolds number [-]

Greek symbols

ρ density [kg/m^3]
ν kinematic viscosity [m^2/s]
μ viscosity [Pa s]
α solid phase volume fraction [-]

Subscripts

l liquid
p particle
z z-component
D drag
l lift
w wall
td turbulent dispersion

REFERENCES

[1] S. Antal, R.Lahey Jr., J. E. Flaherty, "Analysis of phase distribution in fully developed laminar bubbly two-phase flow", International Journal of MultiphaseFlow, vol. 17, No. 5, 635–652, 1991.

[2] M. De Bertodano, R. Lahey,O. Jones, "Phase distribution in bubbly two-phase flow in vertical ducts", International Journal of Multiphase Flow, Vol. 20 No. 5, 805–818, 1994.

[3] A. Troshko, A. Hassan, "A two-equation turbulence model of turbulent bubbly flows", International Journal of Multiphase Flow,Vol. 2, No.11, 1965–2000. 2001.

[4] A. Tomiyamaa, H. Tamaia, I. Zunb, S. Hosokawaa, "Transverse migration of single bubbles in simple shear flows", Chemical Engineering Science, Vol. 57, No. 11, 1849–1858. 2002.

[5] D. Lucasa, E. Kreppera, H. Prasserb, "Use of models for lift, wall and turbulent dispersion forces acting on bubbles for poly-disperse flows", Chemical Engineering Science, Vol. 62, No. 15, 4146–4157,2007.

[6] R. Rzehak, E. Krepper, C. Lifante, "Comparative Study of Wall-Force Models for the Simulation of Bubbly Flows", Nuclear Engineering and Design, Vol. 253, 41–49, 2012.

[7] H. Monji, B. Oesterle, P. Boulet, G. Matsui , " Numerical simulation of nearly equally Density solid-liquid tow-phase flow in a horizontal pipe", International Conference on Multiphase Flow, New Orleans, LA, U.S.A., 2001.

[8] A. AL Jarrah**, "**Phase Distribution of Nearly Equal Density Solid-Liquid Tow Phase Flow in a Horizontal Pipe: Experimental and modeling",Journal of Mathematics and Technology, Vol. 2. No.1, February, 2011.

[9] M. Lance, M. De Bertodano, "Phase distribution phenomena and wall effects in bubbly two-phase flows", Multiphase Science and Technology, Vol. 8, 1-4. 1994.

[10] S.Hosokawa, A.Tomiyama, S. Misaki, T.Hamada , "Lateral Migration of Single Bubbles Due to the Presence of Wall, ASME 2002 Joint U.S.-European Fluids Engineering Division

Conference', Volume 1: Fora, Parts A and B, Montreal, Quebec, Canada, 14–18. 2002.

[11] Fluent Inc., " Fluent 6.3 User's Guide", Fluent 2006.

[12] F. J. Moraga, A. E. Larreteguy, D. A. Drew, R. T. Lahey, "Assessment of Turbulent Dispersion Models for Bubbly Flows", International Conference on Multiphase Flow, New Orleans, LA, U.S.A., 2001.

[13] C. A. Coulaloglou, L. L. Tavlarides "Drop Size Distributions and Coalescence Frequencies of Liquid-Liquid Dispersions in Flow Vessels", AIChE, Vol. 22, No.2, 289-297, 1976.

[14] M. Ishii, N. Zuber, " Drag-Coefficient and Relative Velocity in Bubbly, Droplet or Particulate Flows", AICHE J., Vol. 25, No2, 843-858, 1979.

[15] T.H. Shih, W. W. Liou, A. Shabbir, Z. Yang, and J. Zhu., " A New-Eddy Viscosity Model for High Reynolds Number Turbulent Flows - Model Development and Validation", Computers Fluids, Vol. 24, No. 3,227-23, 1995.

[16] M. S. Politano, P. M. Carrica, J. A. Converti, "A Model for Turbulent Polydisperse Two-Phase Flow in Vertical Channels", International journal of Multi Phase Flow, Vol 29, No.3, 1153-11820, 2003.